

Review

# Vegetation Index Research on the Basis of Tree-Ring Data: Current Status and Prospects

Tongwen Zhang <sup>1,\*</sup> , Jinghui Song <sup>2,3</sup>, Yuting Fan <sup>3,\*</sup> , Yan Liu <sup>3</sup>, Shulong Yu <sup>3</sup>, Dong Guo <sup>3</sup>, Tianhao Hou <sup>4</sup> and Kailong Guo <sup>4</sup>

<sup>1</sup> Xinjiang Uygur Autonomous Region Climate Center, Urumqi 830002, China

<sup>2</sup> College of Geography and Remote Sensing Sciences, Xinjiang University, Urumqi 830046, China; songjh@stu.xju.edu.cn

<sup>3</sup> Institute of Desert Meteorology, China Meteorological Administration, Urumqi 830002, China; liuyan@idm.cn (Y.L.); yushl@idm.cn (S.Y.); guodong@idm.cn (D.G.)

<sup>4</sup> School of Geography and Tourism, Xinjiang Normal University, Urumqi 830054, China; houtianhao@stu.xjnu.edu.cn (T.H.); guokailong@stu.xjnu.edu.cn (K.G.)

\* Correspondence: zhangtw@idm.cn (T.Z.); fanyt@idm.cn (Y.F.)

**Abstract:** The normalized difference vegetation index (NDVI) and tree-ring parameters are commonly used indicators in the research on forest ecology and responses to climate change. This paper compiles and analyzes the literature on vegetation index research on the basis of tree-ring information in the past 20 years and provides an overview of the relationship between tree-ring parameters and NDVI, as well as NDVI reconstruction. The research on the vegetation index based on tree-ring data is mainly concentrated in the middle and high latitudes, and relatively few studies are concentrated in the low latitudes. The tree-ring parameters have a strong correlation with the NDVI in the summer. In terms of tree-ring reconstruction NDVI, *Sabina przewalskii* is the tree with the longest reconstruction sequence so far, and the tree-ring width is the main proxy index. In addition, combining tree rings with the NDVI is useful for assessing forest decline, quantifying the forest response to drought, and monitoring forest productivity. In the future, it is necessary to consider a variety of environmental factors to find the optimal model construction parameters and carry out research on the climate response of forest tree growth and the reconstruction of the historical sequence of the vegetation index at large spatial scales.

**Keywords:** tree ring; vegetation index; tree-ring reconstruction; research progress



**Citation:** Zhang, T.; Song, J.; Fan, Y.; Liu, Y.; Yu, S.; Guo, D.; Hou, T.; Guo, K. Vegetation Index Research on the Basis of Tree-Ring Data: Current Status and Prospects. *Forests* **2023**, *14*, 2016. <https://doi.org/10.3390/f14102016>

Academic Editor: Jesús Julio Camarero

Received: 22 August 2023

Revised: 4 October 2023

Accepted: 5 October 2023

Published: 8 October 2023



**Copyright:** © 2023 by the authors. Licensee MDPI, Basel, Switzerland. This article is an open access article distributed under the terms and conditions of the Creative Commons Attribution (CC BY) license (<https://creativecommons.org/licenses/by/4.0/>).

## 1. Introduction

Vegetation growth and distribution are closely related to climate change. Revealing the relationship between vegetation activity and climate change and its response pattern has become an important part of current global change research, providing a theoretical basis for coping with climate change and improving the sustainable development ability of ecosystems. Working Group I of the Sixth Assessment Report of the Intergovernmental Panel on Climate Change (IPCC, 2021) reported that the global average atmospheric temperatures and ocean temperatures are increasing, and this is leading to the widespread melting of snow and ice and global sea level rise [1]. Climate change is thought to be a major driver of vegetation growth and forest productivity. Tree-ring parameters and the normalized difference vegetation index (NDVI) are commonly used indicators in studies of forest ecology and responses to climate change [2–4]. Tree-ring parameters integrate abiotic (climatic and site conditions) and biotic (ecophysiological responses) factors to provide long-term historical information on the physiological processes of tree growth and responses to environmental changes at an annual time resolution [5–7]. Tree-ring parameters have been widely used in both small-scale climate response studies and large-scale reconstruction studies for their various advantages, including their ability to

yield accurate date information, their high continuity and temporal resolution, their wide availability, and the ease with which several copies of tree rings can be obtained [8,9]. The main advantages of NDVI data on the basis of remote sensing satellite data are the ease with which these data can be acquired, their wide coverage, and their temporal resolution, which permits vegetation growth to be detected over larger areas [10–12]. However, the collection of remote sensing vegetation index data has a short history. The longest sequence of such data is a dataset, which has been provided by AVHRR since 1980. Given that obtaining a sequence of vegetation phenological parameters over the past hundred years is not possible [13,14], data that can serve as a proxy for vegetation change are important for the long-term monitoring of land surface characteristics and studies of climate and terrestrial ecosystem changes.

The growth process of trees can be divided into the primary growth of germination, flowering, branch, leaf, and root derivative growth and the secondary growth of the trunk, branch, and root [15,16]. During the growth process, trees are not only affected by their own factors, but also by external environmental factors [17,18]. As one of the important indicators of tree growth, tree-ring parameters such as the width, density, and stable isotope can continuously record the changes in the external climate and environment in the secondary growth process of trees and quantitatively display the changes in the climate and environment [19,20]. The remote sensing vegetation index can quantify the changes in the leaf area and greenness in the tree canopy. Leaves are the main organs of photosynthesis, and their growth conditions determine the material mass required for the radial growth of trees, reflecting the growth of trees from different levels [21]. In the past, scholars mainly used tree-ring data to reconstruct past climate changes or studied tree ring and vegetation dynamics separately. In recent years, domestic and foreign scholars have begun to combine tree-ring data with remote sensing data for research. The results show that when tree growth and regional vegetation are affected by common external environmental factors, and not affected by other non-climatic factors, the mathematical relationship between the tree-ring and NDVI in the same area and time period can be established. This can effectively deduce the change in the NDVI index in a historical period. With the increasing importance of tree-ring data in the analysis of long-term vegetation dynamic change, there have been studies that calculated the correlation between different vegetation index indicators and the tree-ring index. However, on a global scale, the response of forest growth to NDVI has a very high spatial and temporal diversity. Therefore, it is necessary to review the existing literature on tree rings and NDVI to find the relationship between tree-ring parameters and the vegetation index. Combining tree-ring data with remote sensing data can aid in our understanding of the factors affecting vegetation change; these data can also facilitate the identification of climatic events leading to vegetation change and improvements in the parameters of the global vegetation index reconstruction model. Here, we summarize the historical and recent vegetation index research on the basis of tree-ring data with a focus on tree-ring parameters, forest types, remote sensing data at different spatial resolutions, and future research directions to provide a reference for future research. Figure 1 shows the spatial distribution of sampling points for vegetation index research on the basis of tree-ring data.

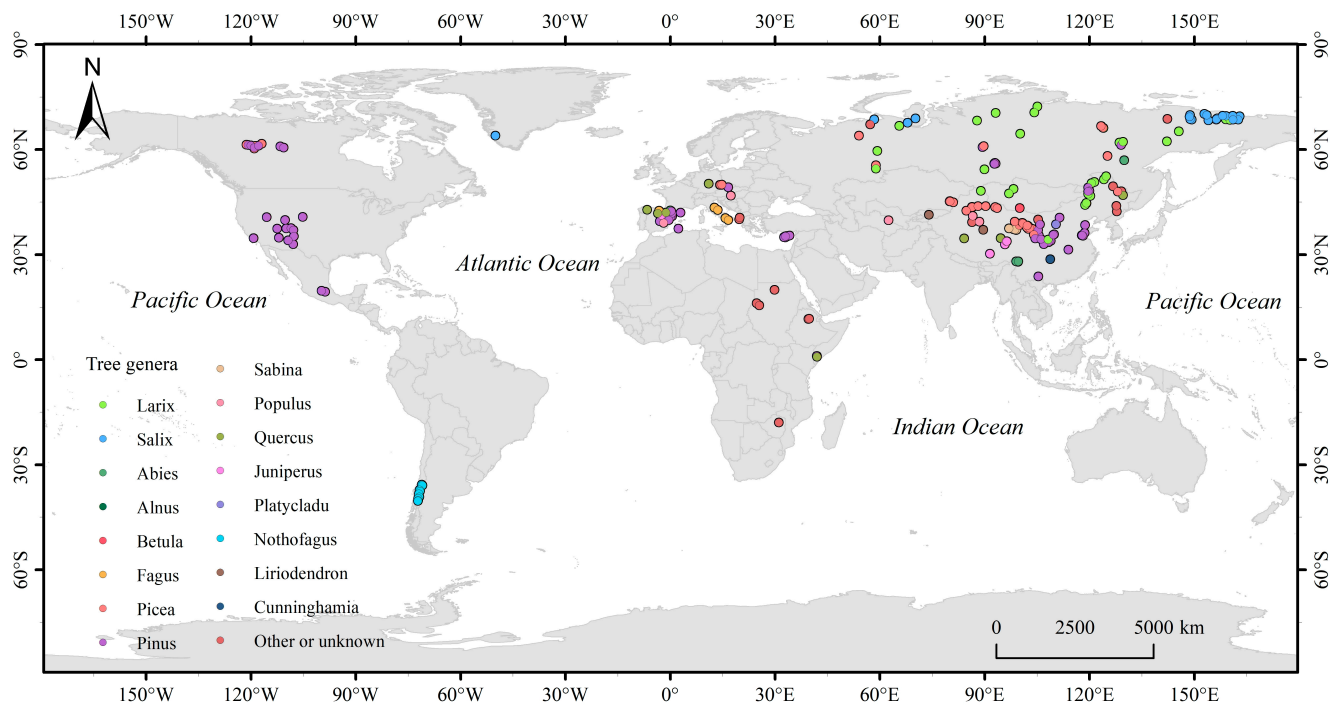


**Figure 1.** Distribution of sampling points of vegetation index studies on the basis of tree-ring data.

## 2. Study of the Relationships between Tree-Ring Parameters and Vegetation Index

An analysis of the relationships between tree-ring parameters and remote sensing data generally involves using tree-ring data to establish a long time series of vegetation change. Research employing tree-ring parameters combined with remote sensing data began in the late 1990s [22]. Tree-ring data have been used to test the reliability of models for estimating net primary productivity values; researchers initially explored the potential and limitations of tree-ring parameters in studies of vegetation productivity [23]. Some studies have detected strong correlations between tree-ring indexes and vegetation indexes (e.g., NDVI), and long-term sequences of vegetation change have been reconstructed on the basis of significant correlations [24–27]. Some studies have also shown that tree-ring parameters are decoupled from NDVI [28,29], and that many factors can affect the relationship between tree radial growth and the vegetation canopy, including the forest type, latitude, elevation, topography, and the spatial resolution of remote sensing data [30–38]. Therefore, the factors and processes affecting the relationship between tree-ring parameters and vegetation indexes are complex. All of the above results indicate that the relationship between tree-ring parameters and NDVI deserves further research.

### 2.1. Relationship between Tree-Ring width and Vegetation Index

Approximately 77.4% of NDVI and tree-ring width parameters are synchronized (i.e., positively correlated) during the growing season in arid regions of inland Asia. On the monthly scale, 69.4% of the maximum correlation coefficients between the NDVI and tree-ring width were concentrated in the period of May–July, especially in June [39]. This indicates that there is a strong synchronization between NDVI and the tree-ring width index from May to July [40]. This synchronous pattern has also been observed in many studies in the Northern Hemisphere. For example, the radial growth of trees in a semi-arid grassland in North China was found to be positively correlated with NDVI in the grassland from early May to early July [41]. Tree-ring width chronology was found to be positively correlated with the growing season NDVI and annual NDVI, and the correlation with the cumulative NDVI from June to October was the strongest [42]. There was a correlation between the tree-ring width and early-spring NDVI and late-autumn NDVI in the area south of 40° N. However, in the area north of 40° N, there was a correlation between the

tree-ring width and NDVI in the summer, and the correlation between the tree-ring width and NDVI varied greatly among the months because of variation in the environmental conditions [43]. A low correlation was found between the tree-ring width chronology and NDVI from May to August in the Hejigong Mountain area of Nanzheng County, which mainly stemmed from differences in vegetation growing seasons caused by latitudinal differences [44]. The upper limit of the tree-ring width index was positively correlated with the NDVI in June, but no significant correlation was observed in July and August, when the vegetation growth was the most vigorous [45,46]. This might stem from the fact that cell division and expansion in several types of conifers ceased in June; although changes in the tree radial width were negligible, the vegetation canopy continued to grow, which resulted in a continuous increase in the regional NDVI value and in a weak correlation between the tree-ring width and NDVI from July to October. This indicates that accurate information on the tree radial growth and measurements of vegetation indexes at a high spatial resolution are necessary for clarifying the relationships between tree-ring parameters and the NDVI.

In areas dominated by snow that rarely melt in winter, snow can reflect large amounts of visible and red wavelengths and absorb near-infrared waves, which makes the calculated NDVI negative and reduces the NDVI value in the study area. However, winter precipitation provided sufficient water for tree-ring growth in the following year; consequently, the tree-ring width was negatively correlated with the NDVI in the non-growing season [47]. The relevant literature indicates that there is a weak or no correlation between the NDVI and tree-ring width in some areas [48]. For example, a weak correlation between the poplar tree-ring width and NDVI was found in the Tarim River, Xinjiang [16]. There was no common relationship found between the radial growth and NDVI of Norwegian spruce trees [49]. There was no significant correlation between the NDVI and tree-ring width at four Arctic tree system sites in North America [29]. The variation in the tree-ring width in Canada was not found to be consistent with the variation in the NDVI, and the reasons for this result remain unclear. This suggests that tree growth is not always correlated with the NDVI [50]. In addition, the scarcity of trees in the study area might explain why the NDVI data reflect both the canopy conditions of trees, as well as the canopy conditions of understory vegetation, thus leading to an increase in the NDVI and a decrease in the tree-ring width near the forest line in northern Russia in summer [51].

## *2.2. Relationship between Tree-Ring Density, Stable Isotope, and Vegetation Index*

Because of the rapid development of modern science and technology and the use of new experimental equipment, the tree-ring width is no longer the only source of data for vegetation index research. The tree-ring density, tree-ring cell structure, and tree-ring stable isotopes have also begun to be used in studies of tree rings combined with remote sensing data. The tree-ring density index reflects the tree cell wall thickness, cell lumen area, and volume and provides indirect information on the tree hydraulic characteristics, carbon sequestration, and paleoclimate records [52,53]. Research on the tree-ring density combined with remote sensing data began in 2000. The chronology of the tree-ring maximum density was found to be negatively correlated with the NDVI in the summer and positively correlated with the NDVI in the late spring and early summer [23]. Current studies on the relationship between tree-ring data and the NDVI are mostly limited to analyses of certain tree-ring parameters. Researchers have analyzed the relationship between seven tree-ring parameters and NDVI and found that the maximum density of tree rings was highly correlated with NDVI. A significant variation was observed in the relationship between tree-ring data and remote sensing data [54]. The relationships of MODIS NDVI, MODIS EVI, and MODIS LAI with the minimum tree-ring density, average tree-ring density, and maximum tree-ring density were studied in two regions with similar climate, soil, and vegetation. The maximum density of tree rings in one region was strongly positively correlated with NDVI in March; the NDVI was negatively correlated with the minimum density of tree rings, and this was in contrast to the relationship observed between the NDVI and the average density of tree rings. This suggests that the tree-ring

density and remote sensing information should be used to understand forest responses to climate change [30]. The relationship between the maximum tree-ring density and NDVI was found to be consistent with the relationship between the tree-ring width index and NDVI in temperature-restricted study areas [55]. There was a significant positive correlation between the tree-ring maximum density chronology and NDVI during the growing season. In the tundra–forest transition zone, the maximum tree-ring density and tree-ring width index were closely related to the NDVI in the growing season [56].

In terms of tree-ring carbon isotopes, to determine the NDVI and tree-ring parameters that are most suitable for forest carbon uptake research, the tree-ring width, tree-ring carbon isotopes, and NDVI were compared with the gross primary productivity (GPP) estimates using the vorticity covariance method. The tree-ring parameters were significantly positively correlated (tree-ring width) and negatively correlated (stable carbon isotope ratio ( $\delta^{13}\text{C}$ )) with the GIMMS NDVI in June and from June to August, and a 1-year lag effect was observed [57]. There were also strong correlations between the tree-ring width, tree-ring carbon isotope, and total forest primary productivity [58,59]. The forest carbon uptake can be more easily studied using tree-ring parameters than using satellite vegetation indexes [60,61]. In a previous study, the researchers explored the effects of volcanic activity on tree growth using stable ring isotopes from surviving trees that grew near the pre-eruption NDVI enhanced area of Mount Etna. The study found that additional soil water condensed by degassed water vapor promoted photosynthesis, leading to a local increase in the NDVI on Mount Etna's flanks prior to the 2002/2003 eruption. Other studies have shown that stable oxygen isotopes in tree rings can be used as indicators of past volcanic eruptions [62]. Insects can affect vegetation photosynthesis by depleting leaf epidermal cells and damaging stomatal regulation. Insect outbreaks were found to have a negative effect on poplar tree growth [63]. During insect outbreaks, the summer NDVI was positively correlated with radial growth and negatively correlated with  $\delta^{13}\text{C}$ . Insect dynamics are important for detecting tree growth at large scales. The ratio of carbon and oxygen isotopes was found to be mainly related to the NDVI at the beginning of the previous autumn and winter season and the beginning of the growing season. They also detected a positive correlation between tree-ring stable isotopes and the summer NDVI [31].

### *2.3. Research on the Relationships between Tree-Ring Parameters and Vegetation Indexes at Different Spatial Resolutions*

In areas with complex vegetation types, the NDVI at coarse spatial resolutions tends to ignore heterogeneity in the vegetation landscape, stand density, and age structure, which results in a spatial disconnect between the NDVI and dendrochronology data, thus weakening the relationship between them. The responses of data at a medium spatial resolution (MODIS, 250 m) and coarse spatial resolution (GIMMS3g NDVI, 8 km) to tree growth were compared in Siberia using a random forest model. The MODIS NDVI growth signal in a conifer forest was stronger than that of the GIMMS3g NDVI. Among all the of the NDVI phenological indexes, the correlation between the summer NDVI and tree-ring width was the strongest, followed by the summer NDVI and spring NDVI of the previous year [64]. In contrast to previous studies, the MODIS NDVI (1 km) was used to predict the spatial distribution of tree-ring width from 2001 to 2017, revealed a positive correlation between the tree-ring width index and the period from June to August, and showed that the forest disturbance and restoration process in the study area were both related to hydrodynamics [65]. In addition, the NDVI values were calculated using high-resolution 30 m Landsat data to analyze and compare the climate signals of the leaf biomass and stem biomass under complex terrain. Compared with the NDVI data with a 250 m spatial resolution, the NDVI data with a 30 m spatial resolution did not enhance the correlation between the tree-ring width and NDVI, which indicates that the NDVI data with a 250 m spatial resolution may be sufficient to study the correlation between the tree-ring parameters and NDVI [66]. In addition to remote sensing observation data, phenological cameras and drones, as near-surface observation technologies, have also

become new sources of vegetation data information [67]. Phenologists have found that the effectiveness of remote sensing to extract vegetation information in mountainous areas is much lower than that of phenological cameras. The resolution of vegetation information obtained using a phenological camera is much higher than that of remote sensing data and is less affected by weather, which can realize the observation of single vegetation, and thus improve the extraction and verification accuracy of remote sensing phenological data [68]. Its limitation is that phenological cameras need to be installed on specific fixed devices. The observation range is smaller than that of remote sensing data, and data collection in the region without signal is costly and susceptible to the influence of the observation angle [69]. Therefore, the establishment of operational phenological camera observation standards, and the combination of tree-ring data as well as vegetation data extracted using a phenological camera will be conducive to the reconstruction of a set of long-term stable vegetation data series.

#### 2.4. Relationships between the Tree-Ring Parameters and Vegetation Indexes of Different Forest Types

Vegetation index studies on the basis of tree-ring data have been mostly conducted at middle and high latitudes, and most studies have been conducted on coniferous forests. In recent years, there has been increased interest in the study of the tree rings of broad-leaved trees and shrubs. The tree-ring growth of broad-leaved trees and shrubs in cold regions has a shorter response time to the cumulative NDVI compared with coniferous forests in temperate and arid regions. The correlations between tree-ring parameters and the NDVI of deciduous trees and conifers show virtually no temporal overlap. For deciduous tree species, the tree-ring parameters are mainly correlated with the NDVI in April, May, August, and October, whereas for conifers, the tree-ring parameters are mainly correlated with the NDVI in May, June, and July. This might stem from the different responses of different tree species to climate change. *Pinus sylvestris* var. *mongolica* Litv. was found to be more strongly correlated with the NDVI than *Picea abies*. The correlation between the two was the strongest in the plateau area, followed by the south slope, north slope, and valley. The tree-ring parameters are more closely related to climate factors than the NDVI. This might be affected by changes in biomass allocation during drought, the spectral distortion of remote sensing data, and the effects of different meteorological conditions on the stem and crown [66]. The relationship between the annual forest growth and NDVI were quantified in different forest types and regions. It showed that 67% of the global forest NDVI was significantly positively correlated with tree-ring growth. There were eight main models between the tree-ring growth and NDVI. The results indicated that the degree of correlation between the NDVI and tree-ring growth was similar in different forest types, and the spatial and temporal diversity of the relationship between forest secondary growth and the NDVI mainly stemmed from differences among tree species and environmental conditions [70]. In addition, high-resolution remote sensing data and the tree-ring parameters of different forest types were studied in Canada. The results showed that the relationships of the tree-ring parameters of cypress (*Thuja*), pine (*Pinus*), and spruce (*Picea asperata* Mast.) with the remote sensing satellite data were closer than the relationships of the tree-ring parameters of oak (*Quercus* L.) and poplar (*Populus* L.) with the remote sensing satellite data. The correlations between the tree-ring width chronology and satellite data were particularly weak for maple (*Acer palmatum* Thunb. in Murray). The negative response of the deciduous tree-ring width to summer air temperatures and the positive response of canopy to summer air temperatures might explain the weak correlation between the two [71]. A VS-oscilloscope model was used to study the relationship between vegetation canopy and trunk cambium phenology. The results showed that the forest canopy was significantly correlated with the end of season of the Chinese pine cambium. And the strength of this correlation was greater than that between grassland and cambium [72]. A significant positive correlation between the NDVI and shrub growth was found in July [73]. A relationship between the interannual variation in the NDVI with the radial growth

of shrubs was detected. A significant positive correlation between the radial growth of shrubs and the summer NDVI were detected in relation to shrub expansion from multiple perspectives. Shrub expansion may be related to the rate of sustained warming in early summer and the frequency of extreme winter warming events [74]. In addition, shrub growth and interannual changes in the NDVI in the Patagonian steppe are regulated by winter precipitation, and tree radial growth explains 23%–62% of the seasonal NDVI changes. However, this study did not identify a clear relationship between the tree radial growth and NDVI in high-altitude mountain areas nor clarify the effect of intensive grazing on shrub growth [75].

### 2.5. Relationships between Tree-Ring Parameters and Vegetation Indexes at Different Altitudes

Altitude affects the relationships between the tree-ring parameters and NDVI mainly through temperature and precipitation. The tree-ring data were combined with remote sensing data to quantify the response of tree growth to climate change at different elevations in Cyprus. This showed that there was no common climate driver between tree-ring chronology and the NDVI in high-altitude forest areas. In the low-altitude arid areas dominated by grassland and shrubland, there was a close relationship between the standardized tree-ring chronology and NDVI, which indicates that trees are not representative of the primary productivity of grassland and shrubland [31,76]. In addition, the tree cores of *Picea schrenkiana* at three altitudes in four areas were collected on the north slope of Tianshan Mountain in China from the west to east, and forest NDVI values were extracted in each study area. The relationship between the tree-ring width index and NDVI were found to be gradually weakened from the west to east, and the positive correlation between them was found to be gradually decreased with altitude. Drought stress may be the main factor affecting the positive correlation between the tree-ring width and NDVI in arid mountainous evergreen coniferous forests [4]. The correlation between the canopy and trunk was found to be gradually decreased with altitude. The correlation coefficient was 0.371 in the alpine region, 0.413 in the valley region, and 0.583 in the desert region [77].

## 3. Other Research

### 3.1. Forest Decline

Forest decline has received much research attention, and is characterized by the loss of leaf biomass, the dieback of branches, and even tree death. These changes alter the structure, composition, and function of forests, as well as their response to climate change. Assessing the risk of forest decline is becoming increasingly important for sustainable forestry management as environmental change intensifies. However, given the complexity of the interactions between multiple processes, quantifying the various factors that affect forest decline remains a major challenge. Topographic patterns of the forest growth decline of *Pinus densiflora* in the Mengshan region of eastern China were studied and analyzed, and forest degradation events were identified from 2009 to 2014 using the NDVI and tree-ring width data. A decision tree model was established, and the topographic pattern of forest degradation was characterized. Serious forest degradation was found in this region in 2012, and the altitude factor indirectly determined the vulnerability of forest decline in the study area, indicating that it could be used to predict the risk of spatial decline [32]. Forest decline mainly occurs in five topographic backgrounds: upper slopes and high ridges at low altitudes, U-shaped valleys and upper slopes at high altitudes, and north and northwest directions at high altitudes [78–81]. In addition, repeated dieback and forest decline occurred in southwestern Hungary, and the summer water supply was the main factor limiting black pine growth [82–84]. During three consecutive droughts over the past few decades (1992–1993, 2000–2003, and 2011–2012), black pine was found to be a major contributor to growth. Black pine (*Pinus nigra* Arn.) is becoming less resilient, and the possibility that it might be a future alternative tree species in the Alps and Mediterranean should be reconsidered, given that other species that are better adapted to drought may exist [85].

### 3.2. Extreme Climate Events

Drought and climate warming will place increasing pressure on forests, and severe water scarcity will reduce the photosynthesis and growth rate of trees, thus harming the function of trees, limiting their radial growth, and leading to the formation of narrow or false rings. Linking historical drought to the tree-ring width can help to quantify the response of a forest to drought and predict its vulnerability to future extreme climate events [86]. The canopy height was used to characterize forest drought resistance, and forests with a medium canopy height (ca. 18 m) were found to have the strongest resistance to severe drought. Trunk growth and leaf growth were positively correlated with the canopy coverage of smaller trees (<18 m) and negatively correlated with the canopy coverage of taller trees (>18 m). Tree mortality was negatively correlated with the canopy coverage of smaller trees (<18 m) [87]. An analysis using the NDVI, cumulative NDVI, dendrochronology, water consumption, ecological flow regime, and groundwater depth data was conducted in the middle reaches of the Tarim River. There was a significant correlation between the tree-ring chronology and cumulative NDVI, and strategies for achieving potentially sustainable groundwater depths (−2.3 to −3.7 m) and discharge volumes ( $3.53$  to  $5.90 \times 10^8$  m<sup>3</sup>) that could further promote vegetation growth were proposed [88].

In temperate forests, a late spring frost is a sudden and severe drop in temperature during mild weather, which can negatively affect tree productivity and growth. Large-scale remote sensing data were combined with tree-ring data to detect the magnitude of late spring frost and evaluate the recovery time. The EVI was found to be a more sensitive indicator than the NDVI [89]. The NDVI was used to determine the locations of undamaged, weakly damaged, and severely damaged areas in the study area. Reliability tests were conducted on the tree damage classification using tree-ring data. The NDVI data could be used to remotely monitor the degree of damage to trees caused by insects in cedar forests [90]. In addition, the tree cytology, quantitative wood anatomy, tree-ring width, and remote sensing data were used to conduct the first large-scale reconstruction of the spatio-temporal dynamics of past insect outbreaks [91].

The resilience of forests to drought may vary among biomes. For example, biomes were selected from Mediterranean, temperate, and continental regions and on the basis of previously collected tree-ring and remote sensing data during and after four major droughts (1986, 1994–1995, 1999, and 2005). It was noted that the tree-ring parameters were positively correlated with the NDVI. The tree-ring width index is more sensitive to forest drought resistance than the NDVI data. Semi-arid Mediterranean forests dominated by evergreen gymnosperms had the lowest drought resistance, but a higher recovery rate than humid temperate forests dominated by deciduous angiosperms [92]. Deciduous trees are more susceptible to drought over short (1–3 months) and medium timescales than most evergreen conifers. In addition, to explore the sensitivity of Central Europe's major deciduous tree species, beech (*Fagus sylvatica*) and oak (*Quercus robur*), a principal component gradient analysis, the tree-ring parameters, and remote sensing data were used to quantify the drought sensitivity of tree growth. The results showed that there was a positive correlation between the NDVI and tree-ring width in the spring. Beech is more sensitive to drought events than oak [93].

### 3.3. Research on Forest Productivity on the Basis of Tree-Ring Data

A time series of field-measured tree rings along with remote sensing data can be used to generate a database for assessing spatial and temporal variability in forest productivity. Previous studies have demonstrated the utility of satellite remote sensing data and tree-ring series for monitoring tree productivity [23,42]. The NPP of trees increased significantly with tree age [94]. Tree radial growth, NDVI, and gross forest primary productivity under different environmental conditions in Spain were analyzed, which revealed a positive correlation between the annual NDVI and tree radial growth. The tree radial growth was most strongly correlated with the cumulative NDVI from June to October. And the

tree radial growth and gross forest primary productivity were correlated. This study was the first attempt in Spain to study forest productivity on the basis of tree-ring data in various forest types under different environmental conditions [36]. To explore whether tree-ring stable isotopes can be used as alternatives to NPP, stable isotope ages at four sites were compared in three different hydroclimatic environments in the eastern United States with NPP products at three different temporal and spatial resolutions. Tree-ring stable isotopes can be useful for reconstructing NPP at large scales and over long periods [95]. The correlation between tree-ring stable isotopes and GPP was found to be stronger than that between the tree-ring width and GPP [96]. In addition, tree-ring data have been used to calibrate NPP values on the basis of model estimates. Previous studies have found that the tree-ring width can be used to calibrate models, and dominant tree species and old trees in the study area should be selected when using tree-ring data for model testing [97]. These results suggest that combining canopy and trunk growth studies is necessary for assessing forest productivity.

To sum up, studies on the vegetation index based on tree-ring data are mainly concentrated in the middle and high latitudes, and relatively few studies are conducted in the low latitudes. Tree-ring parameters have a strong correlation with the NDVI in the summer. The results showed that the NDVI of the previous year correlated better with the tree-ring parameters than the current year in forests in eastern North America and Tasmania, whereas this finding suggests that the accumulation of the NDVI from previous year to September in the current year showed a stronger predictive capacity of tree growth. This pattern was mainly found in the forests of Central and South Asia, southern Canada, the Northern USA and Siberia. The poor correlation between tree-ring parameters and the NDVI is mainly concentrated in cold biomes. Specifically, this pattern corresponded to the forests from cold biomes, such as those located in the Alps mountains or in the boreal forests in northern Canada and Scandinavia [70].

#### **4. Research on the Reconstruction of Vegetation Change in the Historical Period on the Basis of Tree-Ring Data**

##### *4.1. Vegetation Index Reconstruction of Tree-Ring Data from Single Sample Sites*

NDVI reconstruction on the basis of tree-ring data is achieved by leveraging the high temporal resolution of tree-ring data, establishing regression models according to tree physiological mechanisms, and conducting correlation analyses. These approaches permit the reconstruction of the NDVI over long periods and provide more complete datasets for future studies [25,98]. Most NDVI studies on the basis of tree-ring data have focused on the relationship between the tree-ring width and NDVI. However, few studies have examined NDVI reconstruction using tree-ring data [28,70]. Domestic research on NDVI reconstruction on the basis of tree-ring data began in 2005 [55]. In light of the increasing importance of tree-ring data in the analyses of long-term changes in vegetation, increasing numbers of researchers have used different tree species in different regions to conduct NDVI reconstruction research [36,99].

In most studies of NDVI reconstruction, the tree-ring width data of several sample points are used. The most well-researched areas include the Tianshan Mountains, Qilian Mountains, Helan Mountains, Qinghai–Tibet Plateau, Changbai Mountains, Xingan Mountains, and Qinling Mountains [100]. The results showed that the tree-ring width can reflect the change in the NDVI in the growing season in middle and high latitudes. For example, tree rings were used to reconstruct the NDVI (245 years) from May to July, the NDVI (206 years) from June to September, and the NDVI (163 years) from June to August in the southern mountains of the Badain Jaran Desert [101], Hasi Mountain [102], and Xinglong Mountain [103]. Both the tree-ring width and NDVI had a significant positive correlation with precipitation in the periods of July–August and May–June of last year, and a significant negative correlation with the temperature in the period of May–June of the same year. Due to the common climate influence, the tree-ring width had the strongest correlation with the period of July–August. Based on this relationship, the NDVI (442 years) from July to August

was reconstructed in central Tibet using the standardized tree-ring chronology. The results show that in the past 20 years, with the increase in the NDVI index and the improvement in vegetation conditions, its coefficient of variation increased, and the frequency of extreme events increased, resulting in the increased risk of animal husbandry development in this region [104]. The NDVI (172 years and 162 years) in July was reconstructed in the Taibai Mountain Nature Reserve using the standardized tree-ring chronology of the northern and southern slopes, respectively [105]. The NDVI of the past 339 years was reconstructed by using the tree-ring width chronography of Spruce in Snow Ridge, and the single-particle Lagrange comprehensive track model mixed with the backward track model and wind field analysis showed that the NDVI anomaly was affected by precipitation brought on by westerly winds [106]. The reconstruction of the NDVI on the basis of tree-ring data is not only affected by tree-ring indexes but also by the latitude, altitude, and vegetation type. For example, the NDVI was considered to contain all vegetation information in a region, and the physiological processes of different vegetation types vary. Therefore, an analysis of the land cover type was conducted, and correlations of the forest NDVI and grassland NDVI with the tree-ring width index were determined. The correlation between the forest NDVI and tree-ring width was stronger than that between the grassland NDVI and tree-ring width, and the summer forest NDVI was reconstructed from 1920 to 2018 [107].

#### 4.2. Vegetation Index Reconstruction on the Basis of Tree-Ring Data

In recent years, large-scale NDVI reconstructions on the basis of tree-ring data have been carried out. For example, the change trend of the NDVI in 193 years was reconstructed according to the tree-ring chronology of *Pinus sylvestris*. The variation in the NDVI in the western Greater Khingan Mountains was analyzed. After the 1950s, the scale and intensity of extreme changes in the NDVI increased significantly, and the effects of human activities on the NDVI were ranked in the order of importance as follows: livestock > afforestation > population > farmland [108]. It is found that there is a significant relationship between the winter and spring NDVI (December to March) and tree-ring index. Based on this significant relationship, the NDVI index of the past 151 years was reconstructed via linear regression. The results showed that the NDVI was lower than average during the 1869–1874, 1886–1889, 1956–1962, and 1975–1980 periods, and recently, the 2000–2004 period, which may be related to low growth and photosynthetic activity [76]. A total of 176 *Picea schrenkiana* were used to establish a regional tree-ring width chronology, and NDVI values over 167 years were reconstructed. And the reconstructed results were compared with historical disaster records and multiple regional climate reconstructions. The NDVI was found to be locally representative as well as reflect the large-scale circulation in Eurasia [26]. In addition, the vegetation changes over the past 377 years were reconstructed using a regression model. It was found that land reclamation policies and farmland conversion projects in historical periods affected the vegetation coverage by affecting the areas of forest land and farmland [98]. To explore whether climate change caused vegetation growth in Western Mongolia, the NDVI and the Siberian larch tree cycle chronology were modeled by using linear regression; meanwhile, the NDVI from 1940 to 2010 was reconstructed. The reconstructed NDVI index did not show a long-term growth trend, which rejects the hypothesis that climate change induced vegetation growth in Western Mongolia [109]. The relationship between the regional NDVI and climate variables and the NDVI and tree-ring width during the growing season (May–October) in the Hulunbuir Grassland were analyzed. The NDVI during the growing seasons in the past 116 years was reconstructed. The results show that the total number of sparse and dense NDVI anomalies in the past 116 years is 22 years. This may be related to Arctic and Pacific climate activity [99].

To improve the reconstruction accuracy, some researchers reconstructed the NDVI using the first principal component of the tree-ring width chronology, tree-ring width chronology of plots, or multiple tree-ring width indexes from tree-ring data. For example, the Ulan difference chronology and Tianjun autoregressive chronology were used to establish a binary regression equation with the grassland NDVI in August, and millennial

changes in the grassland NDVI was reconstructed in the Buha River Basin [110]. It was found that the tree-ring width indexes and NDVI in the Delingha area were greatly affected by the precipitation in June. The tree-ring width indexes' chronology was significantly correlated with the grassland from June to September, and the correlation with NDVI in August was the strongest. So, the first principal component of five tree-ring width index sequences was used to reconstruct millennial changes in the grassland NDVI in August in the Delingha area, which greatly enriches the tree-ring width and vegetation index databases [111]. Through a Pearson correlation analysis, it was found that the NDVI changes in the Qilian Mountains are highly correlated with the first principal component of the five width timelines. The NDVI from June to August over the past 160 years was reconstructed by using the first principal component of the tree-ring difference chronology of five sampling points [112]. The tree-ring width sequences of three sampling points in the study area were combined to establish a regional chronology. And both the NDVI changes in July and the NDVI changes in the grassland from May to July were reconstructed [113]. In addition, the tree-ring chronology and vegetation index data were smoothed to reduce the errors in the tree-ring data and remote sensing observations and increase the accuracy of the reconstructed cumulative NDVI values. It was found that the correlation between the tree-ring width chronology and the NDVI cumulative values of the growing season was significantly enhanced after the tree-ring width chronology and vegetation index data were smoothed [114].

By comparing the above research results, the NDVI reconstruction results were shown to be superior when the first principal component of two timelines was used compared with when the timelines of *Pinus tabuliformis* were used. Comprehensive timelines are superior to the timelines of single sampling sites for reconstructing the NDVI. In addition, when *Picea schrenkiana* was used for NDVI reconstruction, the reconstructed NDVI values were obtained over a longer period and the variance explained was greater when a combination of three sampling points was used compared with when a single sampling point was used. The robustness of the NDVI reconstruction results was higher in high-altitude areas than in low-altitude areas [106,113].

In sum, most studies of NDVI reconstruction have used tree-ring width index data; most studies have also considered multiple factors and used different types of proxy data for comparative verification (historical disaster records, atmospheric circulation, large-scale climate events, temperature reconstruction, precipitation reconstruction, volcanic eruption, and super storms). This approach verifies the reliability of NDVI reconstruction. An analysis of the reconstruction results of different tree species has revealed that most studies were conducted in areas with coniferous forests, and the robustness of the reconstruction results is relatively high. Few studies have reconstructed NDVI values on the basis of the tree-ring width data of broad-leaved forest and shrubs, and cedar is the tree species with the longest reconstructed NDVI time series. Within a certain range, the robustness of the reconstructed NDVI time series increases with the number of sampling points and sample size. However, the results of vegetation index reconstruction vary among regions when different tree species and tree-ring indexes are used. In the future, longer tree-ring chronologies and higher-resolution tree-ring networks should be used to reconstruct several types of vegetation indexes over longer periods and larger areas; this work will provide insights into the processes underlying vegetation changes over long historical periods.

## 5. Conclusions

An analysis of tree-ring parameters, such as the tree-ring width, density, cell, and stable isotopes of different tree species in different habitats, and the data mining of tree-ring samples are needed to enhance our understanding of the relationship between tree-ring data and remote sensing data [115]. The heterogeneity in the vegetation landscape pattern, stand density, age structure, and variation in growth rhythms among different vegetation types can be overlooked when monitoring changes in vegetation via remote sensing, thus weakening the relationship between the tree-ring parameters and vegetation index data.

There is thus a need to consider the spatial matching between remote sensing data and tree-ring data in future research. Fine and accurate UAV technology could be combined with tree-ring data in future research to address this problem. In addition, more than 40 types of vegetation indexes have been defined to date. Vegetation indexes and remote sensing products other than NDVI could be combined with tree-ring data to increase the diversity of reconstruction indexes used. The relationship between tree ring and vegetation index data is affected by tree species, the spatial resolution of remote sensing data, terrain (altitude and slope direction), and other factors [68]. Therefore, multiple environmental factors should be considered to identify the optimal model construction parameters, and multiple sampling points and large sample sizes are ideal. Research on the responses of forest tree growth to climate change and the reconstruction of historical changes in vegetation indexes at large spatial scales will be a major focus of tree ring and vegetation index research in the future.

**Author Contributions:** Conceptualization, T.Z. and J.S.; resources, J.S. and T.H.; writing—original draft preparation, T.Z. and K.G.; writing—review and editing, Y.F.; visualization, Y.L. and D.G.; supervision, S.Y.; project administration, T.Z.; funding acquisition, S.Y. All authors have read and agreed to the published version of the manuscript.

**Funding:** This work was supported by the Desert Meteorological Science Research Foundation of China (Sqj2020002), the Natural Key Research and Development Program (2023YFE0102700), the Natural Science Foundation of Xinjiang Uigur Autonomous Region-Science Fund for Distinguished Young Scholars (2022D01E105), and the Natural Science Foundation of China (41975095).

**Data Availability Statement:** Data sharing is not applicable.

**Conflicts of Interest:** The authors declare no conflict of interest.

## References

1. Masson-Delmotte, V.; Zhai, P.; Pirani, A.; Connors, S.L.; P'ean, C.; Berger, S.; Caud, N.; Chen, Y.; Goldfarb, L.; Gomis, M.I.; et al. *IPCC Summary for Policymakers. Climate Change 2021: The Physical Science Basis. Contribution of Working Group I to the Sixth Assessment Report of the Intergovernmental Panel on Climate Change*; Cambridge University Press: Cambridge, UK; New York, NY, USA, 2023.
2. Berner, L.T.; Massey, R.; Jantz, P.; Forbes, B.C.; Macias-Fauria, M.; Myers-Smith, I.; Kumpula, T.; Gauthier, G.; Andreu-Hayles, L.; Gaglioti, B.V.; et al. Summer warming explains widespread but not uniform greening in the Arctic tundra biome. *Nat. Commun.* **2020**, *11*, 4621. [[CrossRef](#)]
3. Jiang, P.; Liu, H.; Piao, S.; Ciais, P.; Wu, X.; Yin, Y.; Wang, H. Enhanced growth after extreme wetness compensates for post-drought carbon loss in dry forests. *Nat. Commun.* **2019**, *10*, 195. [[CrossRef](#)]
4. Wen, Y.; Jiang, Y.; Jiao, L.; Hou, C.; Xu, H. Inconsistent relationships between tree ring width and normalized difference vegetation index in montane evergreen coniferous forests in arid regions. *Trees* **2021**, *36*, 379–391. [[CrossRef](#)]
5. Granda, E.; Camarero, J.J.; Galván, J.D.; Sangüesa-Barreda, G.; Alla, A.Q.; Gutierrez, E.; Dorado-Liñán, I.; Andreu-Hayles, L.; Labuhn, I.; Grudd, H.; et al. Aged but withstanding: Maintenance of growth rates in old pines is not related to enhanced water-use efficiency. *Agric. For. Meteorol.* **2017**, *243*, 43–54. [[CrossRef](#)]
6. Levesque, M.; Andreu-Hayles, L.; Pederson, N. Water availability drives gas exchange and growth of trees in northeastern US, not elevated CO<sub>2</sub> and reduced acid deposition. *Sci. Rep.* **2017**, *7*, srep46158. [[CrossRef](#)]
7. Marvel, K.; Cook, B.I.; Bonfils, C.J.W.; Durack, P.J.; Smerdon, J.E.; Williams, A.P. Twentieth-century hydroclimate changes consistent with human influence. *Nature* **2019**, *569*, 59–65. [[CrossRef](#)]
8. Zhang, P.; Jeong, J.-H.; Yoon, J.-H.; Kim, H.; Wang, S.-Y.S.; Linderholm, H.W.; Fang, K.; Wu, X.; Chen, D. Abrupt shift to hotter and drier climate over inner East Asia beyond the tipping point. *Science* **2020**, *370*, 1095–1099. [[CrossRef](#)]
9. Büntgen, U.; Allen, K.; Anchukaitis, K.J.; Arseneault, D.; Boucher, É.; Bräuning, A.; Chatterjee, S.; Cherubini, P.; Churakova, O.V.; Corona, C.; et al. The influence of decision-making in tree ring-based climate reconstructions. *Nat. Commun.* **2021**, *12*, 3411.
10. Furusawa, T.; Koera, T.; Siburian, R.; Wicaksono, A.; Matsudaira, K.; Ishioka, Y. Time-series analysis of satellite imagery for detecting vegetation cover changes in Indonesia. *Sci. Rep.* **2023**, *13*, 8437. [[CrossRef](#)]
11. Pompa-García, M.; Vivar-Vivar, E.D.; Sigala-Rodríguez, J.A.; Padilla-Martínez, J.R. What Are Contemporary Mexican Conifers Telling Us? A Perspective Offered from Tree Rings Linked to Climate and the NDVI along a Spatial Gradient. *Remote Sens.* **2022**, *14*, 4506. [[CrossRef](#)]
12. Mao, D.; Wang, Z.; Luo, L.; Ren, C. Integrating AVHRR and MODIS data to monitor NDVI changes and their relationships with climatic parameters in Northeast China. *Int. J. Appl. Earth Obs. Geoinf.* **2012**, *18*, 528–536. [[CrossRef](#)]

13. Fensholt, R.; Proud, S.R. Evaluation of Earth Observation based global long term vegetation trends—Comparing GIMMS and MODIS global NDVI time series. *Remote Sens. Environ.* **2012**, *119*, 131–147. [[CrossRef](#)]
14. Huang, S.; Tang, L.; Hupy, J.P.; Wang, Y.; Shao, G.F. A commentary review on the use of normalized difference vegetation index (NDVI) in the era of popular remote sensing. *J. For. Res.* **2021**, *32*, 1–6. [[CrossRef](#)]
15. Fu, Y.H.; Zhao, H.; Piao, S.; Peaucelle, M.; Peng, S.; Zhou, G.; Ciais, P.; Huang, M.; Menzel, A.; Peñuelas, J.; et al. Declining global warming effects on the phenology of spring leaf unfolding. *Nature* **2015**, *526*, 104–107. [[CrossRef](#)]
16. Wang, L.L.; Gou, X.H.; Xia, J.Q.; Wang, F.; Zhang, F.; Zhang, J.Z. Research progress on cambial activity of trees and the influencing factors. *Chin. J. Appl. Ecol.* **2021**, *32*, 3761–3770.
17. Fang, K.Y.; Chen, Q.Y.; Liu, C.Z.; Cao, C.F.; Chen, Y.J.; Zhou, F.F. Research advances in dendrochronology. *Chin. J. Appl. Ecol.* **2014**, *25*, 1879–1888.
18. Peng, X.M.; Xiao, S.C.; Xiao, H.L. Advances in Methods of Building Tree-ring Width Chronolog. *J. Desert Res.* **2013**, *33*, 857–865.
19. Qi, C.J.; Zhao, Y.L.; Yu, X.L.; Wu, Y. A comprehensive review on dendrochronology. *J. Cent. South Univ. For. Technol.* **2017**, *37*, 1–8.
20. Michelot, A.; Simard, S.; Rathgeber, C.B.K.; Dufrêne, E.; Damesin, C. Comparing the intra-annual wood formation of three European species (*Fagus sylvatica*, *Quercus petraea* and *Pinus sylvestris*) as related to leaf phenology and non-structural carbohydrate dynamics. *Tree Physiol.* **2012**, *32*, 1033–1045. [[CrossRef](#)]
21. Anyamba, A.; Tucker, C.J. Historical perspectives on AVHRR NDVI and vegetation drought monitoring. In *Remote Sensing of Drought. Innovative Monitoring Approaches*; Anderson, M.C., Verdin, J.P., Wardlow, B.D., Eds.; CRC Press: Boca Raton, FL, USA, 2012; pp. 23–49.
22. Malmström, C.M.; Thompson, M.V.; Juday, G.P.; Los, S.O.; Randerson, J.T.; Field, C.B. Interannual variation in global-scale net primary production: Testing model estimates. *Glob. Biogeochem. Cycles* **1997**, *11*, 367–392. [[CrossRef](#)]
23. D’Arrigo, R.D.; Malmström, C.M.; Jacoby, G.C.; Jacoby, G.C.; Los, S.O.; Bunker, D.E. Correlation between Maximum Latewood Density of Annual Tree Rings and NDVI Based Estimates of Forest Productivity. *Int. J. Remote Sens.* **2000**, *21*, 2329–2336. [[CrossRef](#)]
24. Gao, W.D.; Yuan, Y.J.; Zhang, R.B. Reconstruction of Normalized Difference Vegetation Index of Grassland in Hutobi River Basin Based on Tree-Ring. *J. North-East For. Univ.* **2012**, *40*, 26–30.
25. Wang, L.; Ye, M.; Gao, S.; Gou, X.; Xu, Q.; Zhang, T. Effects of hydrothermal factors on vegetation index and tree-ring index of *Populus euphratica* in the lower reaches of the Tarim River. *J. Nanjing For. Univ. Nat. Sci. Ed.* **2017**, *41*, 85–91.
26. Zhang, T.; Zhang, R.; Lu, B.; Mambetov, B.T.; Kelgenbayev, N.; Dosmanbetov, D.; Maisupova, B.; Chen, F.; Yu, S.; Shang, H.; et al. *Picea schrenkiana* tree-ring chronologies development and vegetation index reconstruction for the Alatau Mountains, Central Asia. *Geochronometria* **2018**, *45*, 107–118. [[CrossRef](#)]
27. Li, J.; Wang, S.; Qin, N.; Liu, X.; Jin, L. Vegetation Index Reconstruction and Linkage with Drought for the Source Region of the Yangtze River Based on Tree-ring Data. *Chin. Geogr. Sci.* **2021**, *31*, 684–695. [[CrossRef](#)]
28. Brehaut, L.; Danby, R.K. Inconsistent relationships between annual tree ring-widths and satellite-measured NDVI in a mountainous subarctic environment. *Ecol. Indic.* **2018**, *91*, 698–711. [[CrossRef](#)]
29. Beck, P.S.; Andreu-Hayles, L.; D’Arrigo, R.; Anchukaitis, K.J.; Tucker, C.J.; Pinzón, J.E.; Goetz, S.J. A large-scale coherent signal of canopy status in maximum latewood density of tree rings at arctic treeline in North America. *Glob. Planet. Chang.* **2013**, *100*, 109–118. [[CrossRef](#)]
30. Correa-Díaz, A.; Silva, L.C.R.; Horwath, W.R.; Gómez-Guerrero, A.; Vargas-Hernández, J.; Villanueva-Díaz, J.; Suárez-Espinoza, J.; Velázquez-Martínez, A. From Trees to Ecosystems: Spatiotemporal Scaling of Climatic Impacts on Montane Landscapes Using Dendrochronological, Isotopic, and Remotely Sensed Data. *Glob. Biogeochem. Cycles* **2020**, *34*, e2019GB006325. [[CrossRef](#)]
31. Coulthard, B.L.; Touchan, R.; Anchukaitis, K.J.; Meko, D.M.; Sivrikaya, F. Tree growth and vegetation activity at the ecosystem-scale in the eastern Mediterranean. *Environ. Res. Lett.* **2017**, *12*, 084008. [[CrossRef](#)]
32. Wang, Z.; Lyu, L.; Liu, W.; Liang, H.; Huang, J.; Zhang, Q.-B. Topographic patterns of forest decline as detected from tree rings and NDVI. *CATENA* **2020**, *198*, 105011. [[CrossRef](#)]
33. Montpellier, E.E.; Soule, P.T.; Knapp, P.A.; Shelly, J.S. Divergent growth rates of alpine larch trees (*Larix lyallii* Parl.) in response to microenvironmental variability. *Arct. Antarct. Alp. Res.* **2018**, *50*, e1415626.
34. Oberhuber, W.; Kofler, W. Topographic influences on radial growth of Scots pine (*P. sylvestris* L.) at small spatial scales. *Plant Ecol.* **2000**, *146*, 231–240. [[CrossRef](#)]
35. Vicente-Serrano, S.M.; Gouveia, C.; Camarero, J.J.; Beguería, S.; Trigo, R.; Lopez-Moreno, J.I.; Azorin-Molina, C.; Pasho, E.; Lorenzo-Lacruz, J.; Revuelto, J.; et al. Response of vegetation to drought time-scales across global land biomes. *Proc. Natl. Acad. Sci. USA* **2013**, *110*, 52–57. [[CrossRef](#)] [[PubMed](#)]
36. Vicente-Serrano, S.M.; Martín-Hernández, N.; Camarero, J.J.; Gazol, A.; Sánchez-Salguero, R.; Peña-Gallardo, M.; El Kenawy, A.; Domínguez-Castro, F.; Tomas-Burguera, M.; Gutiérrez, E.; et al. Linking tree-ring growth and satellite-derived gross primary growth in multiple forest biomes. Temporal-scale matters. *Ecol. Indic.* **2019**, *108*, 105753. [[CrossRef](#)]
37. Zhou, Y.; Yi, Y.; Jia, W.; Cai, Y.; Yang, W.; Li, Z. Applying dendrochronology and remote sensing to explore climate-drive in montane forests over space and time. *Quat. Sci. Rev.* **2020**, *237*, 106292. [[CrossRef](#)]
38. Decuyper, M.; Chávez, R.O.; Čufar, K.; Estay, S.A.; Clevers, J.G.P.W.; Prislán, P.; Giricar, J.; Grepinsek, Z.; Merela, M.; de Luis, M.; et al. Spatio-temporal assessment of beech growth in relation to climate extreme in Slovenia—an integrated approach using remote sensing and tree-ring data. *Agric. For. Meteorol.* **2020**, *287*, 107925. [[CrossRef](#)]

39. Wu, Q.Q.; Zhang, X.; Xu, S.X.; Yang, X.H.; Liu, Y.S.; Li, H.Z.; Shi, Z.J. Climatic responses of NDVI and tree growth in the arid areas of inland Asia and their influencing factors. *J. Desert Res.* **2022**, *42*, 1–10.
40. Kaufmann, R.K.; D'arrigo, R.D.; Paletta, L.F.; Tian, H.Q.; Jolly, W.M.; Myneni, R.B. Identifying climatic controls on ring width: The timing of Correlations between the Timing Rings and NDVI. *Earth Interact.* **2008**, *12*, 114. [[CrossRef](#)]
41. Liang, E.Y.; Shao, X.M.; He, J.C. Relationships between tree growth and NDVI of grassland in the semi-arid grassland of north China. *Int. J. Remote Sens.* **2005**, *26*, 2901–2908. [[CrossRef](#)]
42. Wang, J.; Rich, P.M.; Price, K.P.; Kettle, W.D. Relations between NDVI and tree productivity in the central Great Plains. *Int. J. Remote Sens.* **2004**, *25*, 3127–3138. [[CrossRef](#)]
43. Leavitt, S.W.; Chase, T.N.; Rajagopalan, B.; Lee, E.; Lawrence, P.J. Southwestern U.S. tree-ring carbon isotope indices as a possible proxy for reconstruction of greenness of vegetation. *Geophys. Res. Lett.* **2008**, *35*, 33894. [[CrossRef](#)]
44. Wang, R.; Cheng, R.; Xiao, W.; Feng, X.; Liu, Z.; Wang, X. Relationship between Masson pine tree-ring width and NDVI in North Subtropical Region. *Acta Ecol. Sin.* **2011**, *31*, 5762–5770.
45. Guo, Y.F.; Gan, M.; Yang, M.L.; Ta, Z.; Yu, R. Relationship between tree radial growth and normalized difference vegetation index in eastern Tianshan Mountains. *J. Arid. Land Resour. Environ.* **2018**, *32*, 176–180.
46. Yan, P.; Xu, J.N.; Ju, H.; Taben, H.R.; Guo, F.Y.; Mu, X.W.; Ruan, C.Y. A Study on the Relation Between Tree Ring Width Index and NDVI in the Three Parallel Rivers Region, Yunnan Province. *For. Resour. Manag.* **2019**, *6*, 42–48.
47. Liu, J.; Wang, N.; Hou, Y.; Zhang, X.; Chang, J. Analysis on the Correlation between NDVI and Tree-ring Width Chronologies in the Upper Reaches of the Shiyang River. *Arid. Zone Res.* **2012**, *29*, 667–673.
48. Seftigen, K.; Frank, D.C.; Björklund, J.; Babst, F.; Poulter, B. The climatic drivers of normalized difference vegetation index and tree-ring-based estimates of forest productivity are spatially coherent but temporally decoupled in Northern Hemispheric forests. *Glob. Ecol. Biogeogr.* **2018**, *27*, 1352–1365. [[CrossRef](#)]
49. Lawrence, G.B.; Lapenis, A.G.; Berggren, D.; Aparin, B.F.; Smith, K.T.; Shortle, W.C.; Bailey, S.W.; Varlyguin, D.L.; Babikov, B. Climate Dependency of Tree Growth Suppressed by Acid Deposition Effects on Soils in Northwest Russia. *Environ. Sci. Technol.* **2005**, *39*, 2004–2010. [[CrossRef](#)]
50. Girardin, M.P.; Bouriaud, O.; Hogg, E.H.; Kurz, W.; Zimmermann, N.E.; Metsaranta, J.M.; de Jong, R.; Frank, D.C.; Esper, J.; Büntgen, U.; et al. No growth stimulation of Canada's boreal forest under half-century of combined warming and CO<sub>2</sub> fertilization. *Proc. Natl. Acad. Sci. USA* **2016**, *113*, E8406–E8414. [[CrossRef](#)]
51. Berner, L.T.; Beck, P.S.A.; Bunn, A.G.; Goetz, S.J. Plant response to climate change along the forest-tundra ecotone in north-eastern Siberia. *Glob. Change Biol.* **2013**, *19*, 3449–3462. [[CrossRef](#)]
52. Chave, J.; Coomes, D.; Jansen, S.; Lewis, S.L.; Swenson, N.G.; Zanne, A.E. Towards a worldwide wood economics spectrum. *Ecol. Lett.* **2009**, *12*, 351–366. [[CrossRef](#)]
53. Martinez-Meier, A.; Fernández, M.E.; Dalla-Salda, G.; Gyenge, J.; Licata, J.; Rozenberg, P. Ecophysiological basis of wood formation in ponderosa pine: Linking water flux patterns with wood microdensity variables. *For. Ecol. Manag.* **2015**, *346*, 31–40. [[CrossRef](#)]
54. He, J.C.; Wang, L.L.; Shao, X.M. The relationships between Mongolian Scotch pine tree ring indices and normalized difference vegetation index in Mohe, China. *Quat. Sci.* **2005**, *25*, 252–257.
55. Bunn, A.G.; Hughes, M.K.; Kirilyanov, A.V.; Losleben, M.; Shishov, V.V.; Berner, L.T.; Oltchev, A.; Vaganov, E.A. Comparing forest measurements from tree rings and a space-based index of vegetation activity in Siberia. *Environ. Res. Lett.* **2013**, *8*, 035034. [[CrossRef](#)]
56. Andreu-Hayles, L.; D'Arrigo, R.; Anchukaitis, K.J.; Beck, P.S.A.; Frank, D.; Goetz, S. Varying boreal forest response to Arctic environmental change at the Firth River, Alaska. *Environ. Res. Lett.* **2011**, *6*, 045503. [[CrossRef](#)]
57. Tei, S.; Sugimoto, A.; Kotani, A.; Ohta, T.; Morozumi, T.; Saito, S.; Hashiguchi, S.; Maximov, T. Strong and stable relationships between tree-ring parameters and forest-level carbon fluxes in a Siberian larch forest. *Polar Sci.* **2019**, *21*, 146–157. [[CrossRef](#)]
58. Babst, F.; Bouriaud, O.; Papale, D.; Gielen, B.; Janssens, I.A.; Nikinmaa, E.; Ibrom, A.; Wu, J.; Bernhofer, C.; Köstner, B.; et al. Above-ground woody carbon sequestration measured from tree rings is coherent with net ecosystem productivity at five eddy-covariance sites. *New Phytol.* **2013**, *201*, 1289–1303. [[CrossRef](#)]
59. Klesse, S.; Etzold, S.; Frank, D. Integrating tree-ring and inventory-based measurements of aboveground biomass growth: Research opportunities and carbon cycle consequences from a large snow breakage event in the Swiss Alps. *Eur. J. For. Res.* **2016**, *135*, 297–311. [[CrossRef](#)]
60. Dye, A.; Plotkin, A.B.; Bishop, D.; Pederson, N.; Poulter, B.; Hessler, A. Comparing tree-ring and permanent plot estimates of aboveground net primary production in three eastern U.S. forests. *Ecosphere* **2016**, *7*, e01454. [[CrossRef](#)]
61. Teets, A.; Fraver, S.; Hollinger, D.Y.; Weiskittel, A.R.; Seymour, R.S.; Richardson, A.D. Linking annual tree growth with eddy-flux measures of net ecosystem productivity across twenty years of observation in a mixed conifer forest. *Agric. For. Meteorol.* **2018**, *249*, 479–487. [[CrossRef](#)]
62. Seiler, R.; Hajdas, I.; Saurer, M.; Houlié, N.; D'Arrigo, R.; Kirchner, J.W.; Cherubini, P. Tree-ring stable isotopes and radiocarbon reveal pre- and post-eruption effects of volcanic processes on trees on Mt. Etna (Sicily, Italy). *Ecohydrology* **2021**, *14*, e2340. [[CrossRef](#)]

63. A Boyd, M.; Berner, L.T.; Doak, P.; Goetz, S.J.; Rogers, B.M.; Wagner, D.; Walker, X.J.; Mack, M.C. Impacts of climate and insect herbivory on productivity and physiology of trembling aspen (*Populus tremuloides*) in Alaskan boreal forests. *Environ. Res. Lett.* **2019**, *14*, 085010. [[CrossRef](#)]
64. Bhuyan, U.; Zang, C.; Vicente-Serrano, S.M.; Menzel, A. Exploring Relationships among Tree-Ring Growth, Climate Variability, and Seasonal Leaf Activity on Varying Timescales and Spatial Resolutions. *Remote Sens.* **2017**, *9*, 526. [[CrossRef](#)]
65. Xu, P.; Fang, W.; Zhou, T.; Zhao, X.; Luo, H.; Hendrey, G.; Yi, C. Spatial Upscaling of Tree-Ring-Based Forest Response to Drought with Satellite Data. *Remote Sens.* **2019**, *11*, 2344. [[CrossRef](#)]
66. Mašek, J.; Tumajer, J.; Lange, J.; Kaczka, R.; Fišer, P.; Tremml, V. Variability in Tree-ring Width and NDVI Responses to Climate at a Landscape Level. *Ecosystems* **2023**, *26*, 1144–1157. [[CrossRef](#)]
67. Taylor, S.D.; Browning, D.M.; Baca, R.A.; Gao, F. Constraints and opportunities for detecting land surface phenology in dry lands. *J. Remote Sens.* **2021**, *2021*, 9859103.
68. Berra, E.F.; Gaulton, R.; Barr, S. Commercial off-the-shelf digital cameras on unmanned aerial vehicles for multitemporal monitoring of vegetation reflectance and NDVI. *IEEE Trans. Geosci. Remote Sens.* **2017**, *55*, 4878–4886. [[CrossRef](#)]
69. Zahawi, R.A.; Dandois, J.P.; Holl, K.D.; Nadwodny, D.; Reid, J.L.; Ellis, E.C. Using lightweight unmanned aerial vehicles to monitor tropical forest recovery. *Biol. Conserv.* **2015**, *186*, 287–295. [[CrossRef](#)]
70. Vicente-Serrano, S.M.; Camarero, J.J.; Olano, J.M.; Martín-Hernández, N.; Peña-Gallardo, M.; Tomás-Burguera, M.; Gazol, A.; Azorin-Molina, C.; Bhuyan, U.; El Kenawy, A. Diverse relationships between forest growth and the Normalized Difference Vegetation Index at a global scale. *Remote Sens. Environ.* **2016**, *187*, 14–29. [[CrossRef](#)]
71. Bonney, M.T.; He, Y. Temporal connections between long-term Landsat time-series and tree-rings in an urban–rural temperate forest. *Int. J. Appl. Earth Obs. Geoinf.* **2021**, *103*, 102523. [[CrossRef](#)]
72. Li, M.M.; Li, G. Effects of vegetation type on tree ring based NDVI reconstruction for Helan Mountains. *J. Gansu Agric. Univ.* **2020**, *55*, 152–161.
73. Macias-Fauria, M.; Forbes, B.C.; Zetterberg, P.; Kumpula, T. Eurasian Arctic greening reveals teleconnections and the potential for structurally novel ecosystems. *Nat. Clim. Chang.* **2012**, *2*, 613–618. [[CrossRef](#)]
74. Andreu-Hayles, L.; Gaglioti, B.V.; Berner, L.T.; Levesque, M.; Anchukaitis, K.J.; Goetz, S.J.; D’arrigo, R. A narrow window of summer temperatures associated with shrub growth in Arctic Alaska. *Environ. Res. Lett.* **2020**, *15*, 105012. [[CrossRef](#)]
75. Srur, A.M.; Villalba, R.; Baldi, G. Variations in *Anarthrophyllum rigidum* radial growth, NDVI and ecosystem productivity in the Patagonian shrubby steppes. *Plant Ecol.* **2011**, *212*, 1841–1854.
76. Correa-Díaz, A.; Silva LC, R.; Horwath, W.R.; Gómez-Guerrero, A.; Vargas-Hernández, J.; Villanueva-Díaz, J.; Velázquez-Martínez, A.; Suárez-Espinoza, J. Linking remote sensing and dendrochronology to quantify climate-induced shifts in high-elevation forests over space and time. *J. Geophys. Res. Biogeosci.* **2019**, *124*, 166–183. [[CrossRef](#)]
77. Yuan, K.; Xu, H.; Zhang, G. Is There Spatial and Temporal Variability in the Response of Plant Canopy and Trunk Growth to Climate Change in a Typical River Basin of Arid Areas. *Water* **2022**, *14*, 1573. [[CrossRef](#)]
78. Dyer, J.M. Assessing topographic patterns in moisture use and stress using a water balance approach. *Landsc. Ecol.* **2009**, *24*, 391–403. [[CrossRef](#)]
79. Silver, W.L.; Scatena, F.N.; Johnson, A.H.; Siccama, T.G.; Sanchez, M.J. Nutrient availability in a montane wet tropical forest: Spatial patterns and methodological considerations. *Plant Soil* **1994**, *164*, 129–145. [[CrossRef](#)]
80. Gaines, K.P.; Stanley, J.W.; Meinzer, F.C.; McCulloh, K.A.; Woodruff, D.R.; Chen, W.; Adams, T.S.; Lin, H.; Eissenstat, D.M. Reliance on shallow soil water in a mixed-hardwood forest in central Pennsylvania. *Tree Physiol.* **2015**, *36*, 444–458. [[CrossRef](#)]
81. Baldwin, D.C. *Catchment-Scale Soil Water Retention Characteristics and Delineation of Hydropedological Functional Units in the Shale Hills Catchment*; The Pennsylvania State University: State College, PA, USA, 2011; p. 126.
82. Eilmann, B.; Rigling, A. Tree-growth analyses to estimate tree species’ drought tolerance. *Tree Physiol.* **2012**, *32*, 178–187. [[CrossRef](#)]
83. Martin-Benito, D.; Beeckman, H.; Cañellas, I. Influence of drought on tree rings and tracheid features of *Pinus nigra* and *Pinus sylvestris* in a mesic Mediterranean forest. *Eur. J. For. Res.* **2012**, *132*, 33–45. [[CrossRef](#)]
84. Herrero, A.; Zamora, R. Plant Responses to Extreme Climatic Events: A Field Test of Resilience Capacity at the Southern Range Edge. *PLoS ONE* **2014**, *9*, e87842. [[CrossRef](#)]
85. Marqués, L.; Camarero, J.J.; Gazol, A.; Zavala, M.A. Drought impacts on tree growth of two pine species along an altitudinal gradient and their use as early-warning signals of potential shifts in tree species distributions. *For. Ecol. Manag.* **2016**, *381*, 157–167. [[CrossRef](#)]
86. Urrutia-Jalabert, R.; Barichivich, J.; Rozas, V.; Lara, A.; Rojas, Y.; Bahamondez, C.; Rojas-Badilla, M.; Gipoulou-Zuñiga, T.; Cuq, E. Climate response and drought resilience of *Nothofagus obliqua* secondary forests across a latitudinal gradient in south-central Chile. *For. Ecol. Manag.* **2021**, *485*, 118962. [[CrossRef](#)]
87. Xu, P.; Zhou, T.; Yi, C.; Fang, W.; Hendrey, G.R.; Zhao, X. Forest drought resistance distinguished by canopy height. *Environ. Res. Lett.* **2018**, *13*, 075003. [[CrossRef](#)]
88. Ling, H.; Guo, B.; Yan, J.; Deng, X.; Xu, H.; Zhang, G. Enhancing the positive effects of ecological water conservancy engineering on desert riparian forest growth in an arid basin. *Ecol. Indic.* **2020**, *118*, 106797. [[CrossRef](#)]
89. Tonelli, E.; Vitali, A.; Malandra, F.; Camarero, J.J.; Colangelo, M.; Nolè, A.; Ripullone, F.; Carrer, M.; Urbinati, C. Tree-ring and remote sensing analyses uncover the role played by elevation on European beech sensitivity to late spring frost. *Sci. Total. Environ.* **2023**, *857*, 159239. [[CrossRef](#)] [[PubMed](#)]

90. Oguz, C.H.; Ramazan, ö.; Mustafa, A. Monitoring of damage from cedar shoot moth *Dichelia cedricola* Diakonoff (Lep.: Tortricidae) by multi-temporal Landsat imagery. *iForest Biogeosci. For.* **2014**, *7*, 126–131.
91. Prendin, A.L.; Carrer, M.; Karami, M.; Hollesen, J.; Pedersen, N.B.; Pividori, M.; Treier, U.A.; Westergaard-Nielsen, A.; Elberling, B.; Normand, S. Immediate and carry-over effects of insect outbreaks on vegetation growth in West Greenland assessed from cells to satellite. *J. Biogeogr.* **2019**, *47*, 87–100. [[CrossRef](#)]
92. Gazol, A.; Camarero, J.J.; Vicente-Serrano, S.M.; Sánchez-Salguero, R.; Gutiérrez, E.; de Luis, M.; Sangüesa-Barreda, G.; Novak, K.; Rozas, V.; Tiscar, P.A.; et al. Forest resilience to drought varies across biomes. *Glob. Chang. Biol.* **2018**, *24*, 2143–2158. [[CrossRef](#)]
93. Meyer, B.F.; Buras, A.; Rammig, A.; Zang, C.S. Higher susceptibility of beech to drought in comparison to oak. *Dendrochronologia* **2020**, *64*, 125780. [[CrossRef](#)]
94. Buras, A.; Thevs, N.; Zerbe, S.; Wilmking, M. Productivity and carbon sequestration of *Populus euphratica* at the Amu River, Turkmenistan. *For. Int. J. For. Res.* **2013**, *86*, 429–439. [[CrossRef](#)]
95. Levesque, M.; Andreu-Hayles, L.; Smith, W.K.; Williams, A.P.; Hobi, M.L.; Allred, B.W.; Pederson, N. Tree-ring isotopes capture interannual vegetation productivity dynamics at the biome scale. *Nat. Commun.* **2019**, *10*, 742. [[CrossRef](#)] [[PubMed](#)]
96. Diao, H.; Wang, A.; Gharun, M.; Saurer, M.; Yuan, F.; Guan, D.; Dai, G.; Wu, J. Tree-ring  $\delta^{13}\text{C}$  of *Pinus koraiensis* is a better tracer of gross primary productivity than tree-ring width index in an old-growth temperate forest. *Ecol. Indic.* **2023**, *153*, 110418. [[CrossRef](#)]
97. Erasmi, S.; Klinge, M.; Dulamsuren, C.; Schneider, F.; Hauck, M. Modelling the productivity of Siberian larch forests from Landsat NDVI time series in fragmented forest stands of the Mongolian forest-steppe. *Environ. Monit. Assess.* **2021**, *193*, 200. [[CrossRef](#)]
98. Sun, C.; Liu, Y.; Song, H.; Li, Q.; Cai, Q.; Wang, L.; Fang, C.; Liu, R. Tree-ring evidence of the impacts of climate change and agricultural cultivation on vegetation coverage in the upper reaches of the Weihe River, northwest China. *Sci. Total. Environ.* **2019**, *707*, 136160. [[CrossRef](#)]
99. Chen, Z.-J.; Li, J.-B.; Fang, K.-Y.; Davi, N.; He, X.-Y.; Cui, M.-X.; Zhang, X.-L.; Peng, J.-J. Seasonal dynamics of vegetation over the past 100 years inferred from tree rings and climate in Hulunbei'er steppe, northern China. *J. Arid. Environ.* **2012**, *83*, 86–93. [[CrossRef](#)]
100. Wang, H.; Chen, F.; Zhang, R.; Qin, L. Seasonal dynamics of vegetation of the central Loess Plateau (China) based on tree rings and their relationship to climatic warming. *Environ. Dev. Sustain.* **2016**, *19*, 2535–2546. [[CrossRef](#)]
101. Chen, F.; Martín, H.; Zhao, X.; Roig, F.; Zhang, H.; Wang, S.; Yue, W.; Chen, Y. Abnormally low precipitation-induced ecological imbalance contributed to the fall of the Ming Dynasty: New evidence from tree rings. *Clim. Chang.* **2022**, *173*, 13. [[CrossRef](#)]
102. Jia, F.F.; Lu, R.J.; Gao, S.Y. Variations of NDVI recorded by tree-ring in the HASI mountain, the southern margin of the tengger desert. *Quat. Sci.* **2018**, *38*, 327–335.
103. Wang, Y.J.; Ma, Y.Z.; Lu, R.J.; Gao, S.Y. Summer NDVI variability recorded by tree radial growth in the Xinglong Mountain, the eastward extension of the Qilian Mountains, since 1845 AD. *Geogr. Res.* **2016**, *35*, 653–663.
104. Shang, H.M.; Wei, W.S.; Yuan, Y.J.; Yu, S.L.; Zhang, R.B.; Hong, J.C.; Chen, F.; Zhang, T.W.; Fan, Z.A. Normalized vegetation variation index reconstruction based on the tree-ring width in central Tibet. *J. Lanzhou Univ. Nat. Sci.* **2016**, *52*, 18–23.
105. Zhu, X.L.; Li, S.H.; Bai, H.Y.; Hou, L.; Chen, L.; Qin, J. Reconstruction of July NDVI over 172 years based on tree-ring width of *Larix chinensis* in Taibai Mountain Nature Reserve, China. *J. Appl. Ecol.* **2018**, *29*, 2382–2390.
106. Zhang, Q.; Liu, Y.; Li, Q.; Sun, C.-F.; Li, T.; Li, P.; Ye, Y.-D. Reconstruction of summer NDVI over the past 339 years based on the tree-ring width of *Picea schrenkiana* in Bayinbuluke, Central Tianshan, China. *J. Appl. Ecol.* **2021**, *32*, 3671–3679. [[CrossRef](#)]
107. Li, M.-M.; Li, G. Relationship between phenology of vegetation canopy and phenology of tree cambium in Helan Mountains, China. *J. Appl. Ecol.* **2021**, *32*, 495–502.
108. Dong, J.; Yin, T.; Liu, H.; Sun, L.; Qin, S.; Zhang, Y.; Liu, X.; Fan, P.; Wang, H.; Zheng, P.; et al. Vegetation Greenness Dynamics in the Western Greater Khingan Range of Northeast China Based on Dendrochronology. *Biology* **2022**, *11*, 679. [[CrossRef](#)]
109. Hauck, M.; Klinge, M.; Erasmi, S.; Dulamsuren, C. No Signs of Long-term Greening Trend in Western Mongolian Grasslands. *Ecosystems* **2023**, *26*, 1125–1143. [[CrossRef](#)]
110. Wang, Q.C.; Shi, X.H.; Liu, Y.H.; Qin, N.S.; Shao, X.M. Relationship between tree ring indices and vegetation index (NDVI) in Buha river basin, Qinghai. *J. Glaciol. Geocryol.* **2012**, *34*, 1424–1432.
111. He, J.C.; Shao, X.M. Relationships between tree-ring width index and NDVI of grassland in Delingha. *Chin. Sci. Bull.* **2006**, *51*, 1083–1090.
112. Wang, W.Z.; Liu, X.H.; Chen, T.; An, W.L.; Xu, G.B. Reconstruction of regional NDVI using tree-ring width chronologies in the Qilian Mountains, northwestern China. *Chin. J. Plant Ecol.* **2010**, *34*, 1033–1044.
113. Ran, Y.-L.; Chen, Y.-P.; Chen, F.; Zhang, H.-L.; Jia, X.-B. May–July NDVI variation for the middle Qinling Mountains over the past 194 years indicated by tree rings of *Pinus tabulaeformis*. *J. Appl. Ecol.* **2021**, *32*, 3661–3670. [[CrossRef](#)]

114. Zhao, X.Y.; Guo, Y.Y.; Zhu, L.K.; Tian, J.M.; Qu, X.Q.; Ren, J.X.; Li, W.J.; Bu, X.F.; Wang, S.X. Combining remote sensing and tree ring techniques to investigate forest vegetation dynamics and its response to climate change in Yimeng mountainous area from the early 20th century. *J. Earth Environ.* **2020**, *11*, 265–279.
115. Fajstavr, M.; Bednářová, E.; Nezval, O.; Giagli, K.; Gryc, V.; Vavrčík, H.; Horáček, P.; Urban, J. How needle phenology indicates the changes of xylem cell formation during drought stress in *Pinus sylvestris* L. *Dendrochronologia* **2019**, *56*, 125600. [[CrossRef](#)]

**Disclaimer/Publisher’s Note:** The statements, opinions and data contained in all publications are solely those of the individual author(s) and contributor(s) and not of MDPI and/or the editor(s). MDPI and/or the editor(s) disclaim responsibility for any injury to people or property resulting from any ideas, methods, instructions or products referred to in the content.